

Insight into Ramsdellite $\text{Li}_2\text{Ti}_3\text{O}_7$ and Its Proton-Exchange Derivative

Alodia Orera,[†] M. Teresa Azcondo,[†] Flaviano García-Alvarado,[†] Jesús Sanz,[‡] Isabel Sobrados,[‡] Juan Rodríguez-Carvajal,^{§,||} and Ulises Amador^{*,†}

[†]Departamento de Química, Universidad San Pablo-CEU, Urbanización Montepríncipe, Boadilla del Monte, E-28668, Madrid, Spain, [‡]Instituto Ciencia de Materiales de Madrid-CSIC, 28049 Cantoblanco, Madrid, Spain, and [§]Laboratoire Léon Brillouin (CEA-CNRS), Centre d'Etudes de Saclay, 91191 Gif-sur-Yvette, Cedex, France. ^{||} Present address: Institut Laue-Langevin, BP 156-38042 Grenoble, Cedex 9, France.

Received February 26, 2009

Despite being proven to be a good lithium-ion conductor 30 years ago, the crystal structure of the ramsdellite-like $\text{Li}_2\text{Ti}_3\text{O}_7$ has remained uncertain, with two potential models for locating the lithium ions in the structure. Although the model presently accepted states that both lithium and titanium occupy the octahedral sites in the framework, evidence against this model are provided by ^6Li and ^7Li MAS NMR spectroscopy. Thus, about 14% of these octahedral positions are empty since no lithium in octahedral coordination is present in the material. When $\text{Li}_2\text{Ti}_3\text{O}_7$ -ramsdellite is treated with nitric acid a complete exchange of lithium by protons is produced to yield $\text{H}_2\text{Ti}_3\text{O}_7$. The crystal structure of this proton-exchanged ramsdellite has been re-examined combining X-ray diffraction (XRD), neutron powder diffraction (NPD), and spectroscopic (^1H and ^7Li MAS NMR) techniques. Two kinds of protons are present in this material with different acidity because of the local environments of oxygen atoms to which protons are bonded, namely, low acidic protons strongly bonded to highly charged oxygen atoms (coordinated to two Ti^{4+} and a vacancy); and protons linked to low charged oxygen atoms (bonded to three Ti^{4+} ions) which will display a more acidic behavior. $\text{H}_2\text{Ti}_3\text{O}_7$ absorbs water; proton mobility is enhanced by the presence of absorbed water, giving rise to a large improvement of its electrical conductivity in wet atmospheres. Thus, it seems that water molecules enter the tunnels in the structure providing a vehicle mechanism for proton diffusion.

Introduction

In the search for new materials for energy production and storage, lithium titanates (and their derivatives) play an important role. Among them the fast-ion (lithium) conductor ramsdellite- $\text{Li}_2\text{Ti}_3\text{O}_7$ has been used as a solid electrolyte in high-temperature lithium batteries.^{1–4} This compound, and a series of its derivatives,^{5–8} as well as a number of spinel-like lithium titanates, such as $\text{Li}_4\text{Ti}_5\text{O}_{12}$,⁹ have been also reported to be good electrode materials in rechargeable lithium

batteries. Even different titanium oxides show relevant electrochemical activity in a lithium cell.¹⁰ On the other hand, the superconducting properties of LiTi_2O_4 are also well known, though its critical temperature is quite low.¹¹ Finally, $\text{H}_2\text{Ti}_3\text{O}_7$ titanium oxy-hydroxide obtained through proton exchange on ramsdellite- $\text{Li}_2\text{Ti}_3\text{O}_7$ could be a suitable electrolyte for low-temperature fuel-cells for energy production because of its protonic conduction.^{12,13}

The phase $\text{Li}_2\text{Ti}_3\text{O}_7$ with ramsdellite structure, related to that of $\gamma\text{-MnO}_2$,¹⁴ was first reported by Jonkers³ and some years later by Kim et al.¹⁵ Its crystal structure consists of distorted MO_6 octahedra linked up with adjacent octahedra by sharing opposite edges to form columns. Pairs of adjacent columns share edges to form double columns, giving rise to an open framework. In between the double columns there exist channels parallel to the columns, which favors Li mobility, formed by distorted interstitial sites. Although from the pioneering work of Morosin and Mikkelsen,¹⁶ using

*To whom correspondence should be addressed. E-mail: uamador@ceu.es. Phone: 34 91 372 47 35. Fax: 34 91 372 47 12.

(1) Dubey, B. L.; West, A. R. *Nat. Phys. Sci.* **1972**, *23*, 155.
(2) Castellanos, M.; West, A. R. *J. Mater. Sci.* **1979**, *14*, 450.
(3) Jonkers, G. H. *Trabajos de la Reunión Internacional de Reactividad de Sólidos*; Real Sociedad de Química: Madrid 1957.
(4) Boyce, B. J.; Mikkelsen, J. C. *Solid State Commun.* **1979**, *31*, 743–745.
(5) Chen, C. J.; Greenblatt, M. *MRS Bull.* **1985**, *20*, 1347.
(6) Garnier, S.; Bohke, C.; Bohke, O.; Fourquet, J. L. *Solid State Ionics* **1996**, *83*, 323.
(7) Arroyo y de Dompablo, M. E.; Morán, E.; Várez, A.; García-Alvarado, F. *MRS Bull.* **1997**, *32*, 993.
(8) Gover, R. K. B.; Tolchard, J. R.; Tukamoto, H.; Murai, T.; Irvine, J. T. S. *J. Electrochem. Soc.* **1999**, *146*(12), 4348.
(9) Ferg, E.; Gummow, R. J.; de Kock, A.; Thackeray, M. M. *J. Electrochem. Soc.* **1994**, *141*, L147.
(10) Kuhn, A.; Amandi, R.; García-Alvarado, F. *J. Power Sources* **2001**, *92*, 221.

(11) Johnston, D. C. *J. Low Temp. Phys.* **1976**, *25*, 145.
(12) le Bail, A.; Fourquet, J. L. *Mat. Res. Bull.* **1992**, *27*, 75–85.
(13) Corcoran, D. J. D.; Tunstall, D. P.; Irvine, J. T. S. *Solid State Ionics* **2000**, *136-137*, 297–303.
(14) Bystrom, A. M. *Acta Chem. Scand.* **1949**, *3*, 163.
(15) Kim, K. H.; Hummel, F. A. *J. Am. Ceram. Soc.* **1960**, *43*, 611.
(16) Morosin, B.; Mikkelsen, J. C. *Jr. Acta Crystallogr.* **1979**, *B35*, 798.

single crystal X-ray diffraction (XRD), the location of oxygen and titanium was well established, some structural details related to lithium distribution within the structure remained as an open question for years. In ref 16 the authors suggested two extreme models. In model-I all lithium ions are located in distorted tetrahedral sites within the channels, whereas 0.57 octahedral sites in the framework remain vacant. Referring the material's composition to the eight oxygen atoms in the unit cell, the formula for this model is $(\text{Li}_{2.29})_c(\text{Ti}_{3.43}\square_{0.57})_f\text{O}_8$, where c, f, and \square denote channel, framework, and vacancy, respectively. Model-II proposes that all the cation sites in the framework are occupied by titanium and lithium: $(\text{Li}_{1.72})_c(\text{Ti}_{3.43}\text{Li}_{0.57})_f\text{O}_8$.

From neutron powder diffraction (NPD) Abrahams et al¹⁷ claimed that lithium ions are distributed over two of the possible sites previously identified by Grins and West¹⁸ within the tunnels in model-II, proposing also that some lithium ions occupy octahedral sites in the structure framework. However, the evidence given in ref 17 is not conclusive since the sample studied in that paper presented a noticeable amount of an unidentified impurity and the agreement factors given were higher than desirable. A slightly different distribution of lithium ions within the tunnels was reported by Gover and Irvine¹⁹ by combining XRD and NPD data collected on a pure sample, confirming a mixed occupation by Ti and Li of the framework octahedra in $\text{Li}_2\text{Ti}_3\text{O}_7$, but removing any lithium from 8d positions. Interestingly, in a different paper those authors,²⁰ also using neutron and XRD, found no evidence to support a partial occupancy by lithium of octahedral sites in the ramsdellite LiTi_2O_4 . In any case, the model-II proposed by Morosin and Mikkelsen,¹⁶ given by the structural formula $(\text{Li}_{1.72})_c(\text{Ti}_{3.43}\text{Li}_{0.57})_f\text{O}_8$, is presently accepted.

In spite of the above considerations, there is some indirect and direct evidence against this accepted model. Thus, le Bail and Fourquet¹² prepared ramsdellite- $\text{H}_2\text{Ti}_3\text{O}_7$ by direct and complete Li^+/H^+ exchange refluxing ramsdellite- $\text{Li}_2\text{Ti}_3\text{O}_7$ in nitric acid; in the resulting titanium oxi-hydroxide no trace of lithium was found neither by chemical analysis nor by NPD. With this technique, vacant octahedra were detected in the framework of the ramsdellite structure. Thus, it must be assumed that at low temperature lithium ions can be easily removed from the structure framework. Even more, magic angle nuclear magnetic resonance (MAS-NMR) experiments on ramsdellite- $\text{Li}_2\text{Ti}_3\text{O}_7$ ²¹ do not unambiguously confirm the presence of lithium in octahedral coordination.

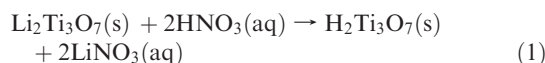
Proton exchange is a suitable method to obtain low temperature proton conductors useful for elaborating membranes for fuel cells. The first titanium oxi-hydroxide was obtained by topotactic exchange of sodium by protons in layered $\text{Na}_2\text{Ti}_3\text{O}_7$.²² Ramsdellite- $\text{H}_2\text{Ti}_3\text{O}_7$ was first reported by le Bail and Fourquet,¹² and its electrical properties were studied by Corcoran et al.¹³ However, previous work on this material left some open questions worthy of study such as the types and acidic characters of

protons, the conductivity in atmospheres of different humidity in relation to the structure, and so on. Since we obtained promising results on other similar systems²³ we decided to study the ramsdellite- $\text{H}_2\text{Ti}_3\text{O}_7$ for such an application. Here, we present a detailed structural re-determination combining XRD, NPD, and spectroscopic techniques (proton and lithium MAS-NMR). In particular we used high-resolution ⁷Li and ⁶Li MAS-NMR spectroscopy to discuss lithium location in ramsdellite- $\text{Li}_2\text{Ti}_3\text{O}_7$. We also present the effect of different humidity atmospheres on the electrical properties of $\text{H}_2\text{Ti}_3\text{O}_7$ obtained by acid treatment, studied by impedance (IS) and ¹H MAS-NMR spectroscopy.

Experimental Section

Samples. Starting $\text{Li}_2\text{Ti}_3\text{O}_7$ ramsdellite was prepared from stoichiometric amounts of anatase- TiO_2 (Aldrich) and Li_2CO_3 (Aldrich). The mixtures were ground and then decarbonated at 1073 K in Pt boats for 24 h. After grinding, the mixture, pellets were made, fired at 1273 K for 48 hours and quenched from this temperature to avoid the ramsdellite-to-spinel phase transition on cooling.²⁴ Portions of this sample were treated to obtain proton-exchanged samples. ⁶Li enriched samples of ⁶ $\text{Li}_2\text{Ti}_3\text{O}_7$ -ramsdellite for NMR experiments were prepared similarly, but using ⁶LiOH·H₂O (Aldrich) as ⁶Li-source. On the other hand, ⁶ $\text{Li}_4\text{Ti}_5\text{O}_{12}$ -spinel used as reference for lithium-site determination was prepared from the same reactants by the procedure described in ref 20.

Ion exchange of lithium by proton was performed, similarly as in ref 12, by refluxing the powdered ramsdellite in a 5 M HNO_3 solution at 353 K for 24 hours (eq 1). Afterwards the resulting powder was isolated by filtration, washed three times with distilled water, and then dried at 333 K under dynamical vacuum for 48 h.



Samples with different amounts of absorbed water were obtained by exposing the sample to a water-saturated atmosphere for different times prior to ¹H MAS-NMR measurements.

Experimental Techniques. All the samples used in this study were checked to be single-phase by powder XRD on a Bruker D8 high-resolution diffractometer, using monochromatic $\text{CuK}\alpha_1$ ($\lambda = 1.5406 \text{ \AA}$) radiation obtained with a germanium primary monochromator, and equipped with a position sensitive detector (PSD) MBraun PSD-50M. The measured angular range, the step size, and the counting times were selected to ensure enough resolution.

The exchanged samples were studied by NPD at room temperature (RT) on the diffractometer G4.2 of the Orphée Reactor at Laboratoire Léon Brillouin. A monochromatic beam of wavelength 2.3390 Å was selected with a Ge(004) monochromator; for this radiation the instrumental resolution is within the range $2.7 \times 10^{-3} \leq (\Delta Q/Q) \leq 0.022$. The structural refinements were carried out by the Rietveld method using the FullProf program.²⁵ Prior to the structure refinements a Le Bail fit²⁶ of the patterns was performed to obtain suitable profile

(17) Abrahams, I.; Bruce, P. G.; David, W. I. F.; West, A. R. *J. Solid State Chem.* **1989**, *78*, 170.

(18) Grins, J.; West, A. J. *Solid State Chem.* **1986**, *65*, 265.

(19) Gover, R. K. B.; Irvine, J. T. S. *J. Solid State Chem.* **1998**, *141*, 365.

(20) Gover, R. K. B.; Irvine, J. T. S.; Finch, A. A. *J. Solid State Chem.* **1997**, *132*, 382.

(21) Kartha, J. P.; Tunstall, D. P.; Irvine, J. T. S. *J. Solid State Chem.* **2000**, *152*, 397–402.

(22) Izawa, H.; Kikawa, S.; Koizumi, M. *J. Phys. Chem.* **1982**, *85*, 5023.

(23) Kuhn, A.; García-Alvarado, F.; Bashir, H.; dos Santos, A. L.; Acosta, J. L. *J. Solid State Chem.* **2004**, *177*, 2366.

(24) Izquierdo, G.; West, A. R. *Mat. Res. Bull.* **1980**, *15*, 1655.

(25) Rodríguez-Carvajal, J. *Physica B* **1993**, *19*, 55. See also a report in CPD of: *IUCr. Newsletter* **26**, (2001) 12; available at: <http://www.iucr.org/iucr-top/comm/cpd/Newsletters>. The program and manual can be found at: <http://www-llb.ccea.fr/fullweb/powder.htm>.

(26) Le Bail, A.; Duroy, H.; Fourquet, J. L. *Mat. Res. Bull.* **1988**, *23*, 447.

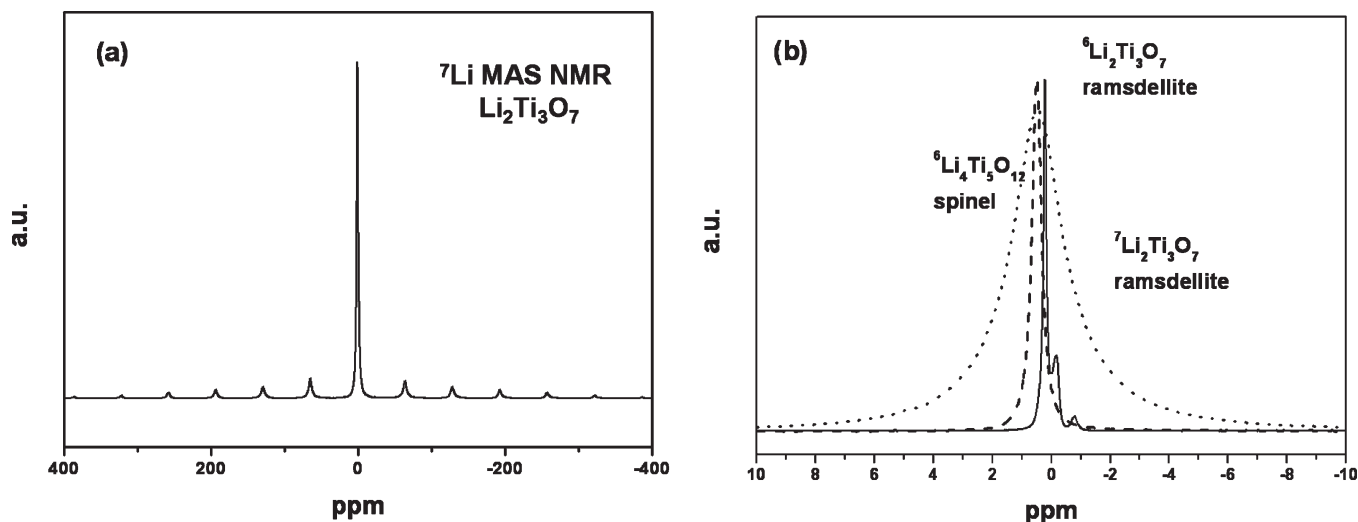


Figure 1. (a) ^7Li MAS-NMR spectrum of the parent compound $\text{Li}_2\text{Ti}_3\text{O}_7$. (b) Comparison of the ^6Li (dashed line) and ^7Li (dotted line) MAS-NMR spectra of the parent ramsdellite- $\text{Li}_2\text{Ti}_3\text{O}_7$. The ^6Li -MAS-NMR spectrum of spinel- $\text{Li}_4\text{Ti}_5\text{O}_{12}$ (continuous line) helps to determine the environment of lithium ions (see text).

parameters. Then, the structural model was refined keeping constant the profile parameters; if needed, along the refinements some of them are allowed to vary, but at the final steps of the refinements they are kept constant. The refinements were stable provided the number of refined parameters describing the structural model was low enough to obtain an adequate peaks-to-parameters ratio. To ensure this, isotropic thermal factors (ITF) were used for all the atoms in the structure, and some structural constraints were imposed. The fitting process was finished when convergence was reached.

Lithium and titanium contents in the parent $\text{Li}_2\text{Ti}_3\text{O}_7$ ramsdellite and in exchanged materials were analyzed by Atomic Absorption Spectroscopy (AAS) in a Varian SpectraAA 220. The samples were solved in a (1:1, v/v) mixture of aqueous H_2O_2 (30% w/v) and concentrated (98%) H_2SO_4 solution of analytical grade. Besides, the lithium content of the exchange solution used to prepare the protonated material was analyzed.

Thermo Gravimetric and Differential Thermal Analyses (TGA and DTA) were carried out in a 200 mL/min stream of pure N_2 in a Seiko TG/DTA 6200 apparatus using about 25 mg and a heating rate of $1.5^\circ\text{C}/\text{min}$ up to a maximum temperature of 1273 K.

Sintering at high temperature is not possible because of the decomposition of the protonated compound. Therefore, pellets of this material were prepared by applying high pressure (20 kbar) in a piston-cylinder press at RT to give pellets of relative densities of about 80%. After conformed, the sample was confirmed by XRD not to suffer any transformation or loss of crystallinity. Impedance spectroscopy measurements were performed on these pellets coated with colloidal silver acting as electrodes by using a FRA Solartron 1260 in the 1 MHz–0.1 Hz range.

^1H , ^7Li , and ^6Li MAS-NMR spectra were recorded with an Avance-400 (Bruker) spectrometer. The frequencies used in this work were 400.13, 155.45, and 58.88 MHz (external magnetic field, 9.4 T). In MAS experiments, the rotor was of Andrew type and spinning rates used were 4 and 10 kHz in proton and lithium signals. Spectra were recorded after a single $\pi/2$ radiofrequency pulse (4 μs). The number of scans amounted to 100, and the interval between scans was chosen to avoid saturation effects (1 s in both signals). In spectra deconvolution, intensity, position, and linewidths of components were determined by using the WIN-NMR (Bruker) software package. However, quadrupolar C_Q and η constants were deduced by a trial and error procedure.

Results and Discussion

$\text{Li}_2\text{Ti}_3\text{O}_7$ Revisited. It is widely accepted that the structural model for $\text{Li}_2\text{Ti}_3\text{O}_7$ -ramsdellite is that proposed by Morosin et al.,¹⁷ slightly modified by Abrahams et al.¹⁸ with the octahedral framework positions shared by Ti^{+4} and Li^+ . However, ^7Li and ^6Li MAS NMR provide evidence against this model. Figure 1a shows the ^7Li MAS-NMR spectrum of the starting ramsdellite; it is formed by a single signal centered at 0.5 ppm and a set of small spinning side bands at both sides of the main signal. The spectral deconvolution revealed the presence of two components centered at 0.5 ppm, displaying different quadrupolar interactions ($^1C_Q \sim 0$ kHz and $^1\eta \sim 0$; $^{11}C_Q \sim 70$ kHz and $^{11}\eta \sim 0.3$). According to these results part of lithium displays an appreciable mobility at RT, the rest being relatively fixed in more distorted sites. Figure 1b shows the central band of the ^6Li MAS-NMR spectrum of a $^6\text{Li}_2\text{Ti}_3\text{O}_7$ -ramsdellite sample, together with a zoomed view of the ^7Li spectrum shown in Figure 1a. The low gyromagnetic ratio and quadrupole moment of ^6Li nuclei decrease considerably the corresponding linewidths (FWHM ca. 25 Hz and basewidth ca. 200 Hz) as a consequence of partial cancellation of dipolar and quadrupolar interactions, improving spectral resolution and allowing site speciation.

The ^6Li spectrum of $\text{Li}_2\text{Ti}_3\text{O}_7$ -ramsdellite consists of one single signal centered at 0.49 ppm, indicating that lithium ions occupy one kind of sites: either octahedral or tetrahedral. In a previous similar ^6Li MAS-NMR study on $\text{Li}_2\text{Ti}_3\text{O}_7$ ¹³ the corresponding spectrum also shows one single sharp line (basewidth ca. 200 Hz). These authors assumed that model-II proposed by Morosin and Mikelsen¹⁶, $(\text{Li}_{1.72})_c(\text{Ti}_{3.43}\text{Li}_{0.57})_d\text{O}_8$, is correct and that the chemical shifts for both tetrahedral and octahedral environments of Li ions are the same.

Fortunately, the ^6Li spectrum of spinel-like $\text{Li}_4\text{Ti}_5\text{O}_{12}$ helps us to assign the signal observed for $\text{Li}_2\text{Ti}_3\text{O}_7$ -ramsdellite. In Figure 1b the ^6Li MAS NMR spectra of ramsdellite- $\text{Li}_2\text{Ti}_3\text{O}_7$ and spinel- $\text{Li}_4\text{Ti}_5\text{O}_{12}$ are compared, for the latter three signals are observed at 0.21, -0.17

Table 1. Refined Structure Parameters for the Parent $\text{Li}_2\text{Ti}_3\text{O}_7$ as Obtained from XRD Data

atom	site ^a	<i>x/a</i>	<i>y/b</i>	<i>z/c</i>	<i>B</i> (Å ²)	occ.
Ti	4c	0.1365(3)	1/4	-0.0296(7)	0.27(4)	0.429
O(1)	4c	0.2698(7)	1/4	0.672(2)	0.26(8)	1/2
O(2)	4c	-0.0346(8)	1/4	0.191(1)	0.26(8)	1/2
Li(1)	8d	0.425(14)	0.132(11)	-0.143(13)	0.26(8)	0.090(4)
Li(2)	4c	0.065(13)	1/4	0.522(11)	0.26(8)	0.188(2)

^a S.G. *Pnma* (62); composition: $\text{Li}_{1.95(2)}\text{Ti}_3\text{O}_7$; $a = 9.5450(2)$ Å, $b = 2.9437(1)$ Å, $c = 5.0154(2)$ Å, $V = 140.92(1)$ Å³. $R_B = 0.079$, $R_{\text{exp}} = 0.065$, $R_{\text{wp}} = 0.089$, $\chi^2 = 1.90$.

and -0.78 ppm. In this spinel it is well established that lithium ions are distributed among tetrahedral (8a) and octahedral (16d) sites in a 3/1 ratio.^{21,27} Thus, in Figure 1b the strongest signal at 0.21 ppm can be ascribed to tetrahedrally coordinated lithium, whereas the weaker one at -0.17 ppm was assigned to Li^+ in octahedral environments. Worthy of note, in over-stoichiometric (lithium intercalated) $\text{Li}_{4+x}\text{Ti}_5\text{O}_{12}$ compounds excess lithium enters empty octahedral holes (16c sites);²⁷ thus, in Figure 1b the third signal at -0.78 ppm indicates that our sample shows a slight but measurable Li over-stoichiometry or disorder. Hence, ⁶Li signals corresponding to tetrahedral lithium in similar titanates appear at more positive chemical shifts than those due to octahedral coordinated ones.^{21,27} Regarding $\text{Li}_2\text{Ti}_3\text{O}_7$ -ramsdellite, the sole signal observed at 0.49 ppm must be due only to lithium tetrahedrally coordinated. Therefore, this result besides indirect chemical evidences commented on below, allowed us to discard the structural model widely accepted, $(\text{Li}_{1.72})_c(\text{Ti}_{3.43}\text{Li}_{0.57})_f\text{O}_8$, and to propose as more likely the alternative one denoted as $(\text{Li}_{2.29})_c(\text{Ti}_{3.43}\square_{0.57})_f\text{O}_8$.

Using the information given by MAS NMR we fitted our XRD data to the refined model of $\text{Li}_2\text{Ti}_3\text{O}_7$ given in Table 1. Figure 2a shows the graphic results corresponding to the fitting of the XRD pattern of starting ramsdellite- $\text{Li}_2\text{Ti}_3\text{O}_7$; the sample is single-phase and chemical analyses give a Ti/Li molar ratio close to the nominal one (3:2). Figure 2b shows the coordination polyhedron of the two lithium sites present in the tunnels of the ramsdellite structure. In both cases lithium is tetra-coordinated to three O(2) and one O(1) defining distorted tetrahedra.

The discrepancy between the composition determined by chemical analysis and that given in Table 1 is not surprising since XRD is not the best technique to deal with structural features related to light atoms such as lithium. Despite this, the fitting of our XRD data was stable and converged to the model presented in Table 1 and depicted in the inset of Figure 2a. Neutron diffraction is much more suited for that; however, even using neutron diffraction, locating lithium in $\text{Li}_2\text{Ti}_3\text{O}_7$ is not easy. Indeed, we simulated NPD patterns (not shown) for both models proposed in ref 16, and the difference in peak intensities is less than 3%, which is lower than the difference between calculated and experimental patterns reported in NPD studies of this material.^{17–20} Even more,

we refined the NPD pattern corresponding to the starting ramsdellite- $\text{Li}_2\text{Ti}_3\text{O}_7$ used in ref 12 to obtain the proton-exchanged material, placed into the public-domain PowBase.²⁸ As for all the other similar structural studies reported, the arguments in favor of model-I $((\text{Li}_{2.29})_c(\text{Ti}_{3.43}\square_{0.57})_f\text{O}_8)$ or model-II $((\text{Li}_{1.72})_c(\text{Ti}_{3.43}\text{Li}_{0.57})_f\text{O}_8)$ are crystallographically weak. For both models similar agreement factors are obtained: $R_B = 0.040$, $R_f = 0.039$, $R_{\text{wp}} = 0.13$, $R_p = 0.146$, and $R_B = 0.042$, $R_f = 0.039$, $R_{\text{wp}} = 0.13$, $R_p = 0.149$, for model-I and II, respectively.

$\text{Li}_2\text{Ti}_3\text{O}_7$ is a good ion conductor, and in spite of its structure showing large tunnels along the *b* axis (Figure 2) it cannot be considered as a one-dimensional (1D) conductor ($\sigma_b/\sigma_a \approx 7$).⁴ In the structural model given by Abrahms et al.,¹⁷ there are up to 12 tetrahedral positions for lithium ions per unit cell inside the tunnels: 8 for Li(1) and 4 for Li(2) (see Table 1). When the structural formula is taken into account, statistical occupancy of these sites is very low, which favors a Li^+ jump from one occupied to an empty position and explaining lithium diffusion along the tunnels (along the *b* axis). Li-NMR results are in agreement with this model: at RT one part of the lithium ions occupy preferentially one kind of tetrahedral site (4c sites) but the other part displays high mobility (8d sites). This seems to contradict the results by Morosin and Mikkelsen¹⁶ who found no thermal diffuse scattering in their single crystal XRD photographs; however, different time scales for NMR spectroscopy and XRD can account for this apparent contradiction. On the other hand, the existence of octahedral vacancies explains the high conductivity values measured along *a* and *c* axes,⁴ since they allow lithium ions to move between tetrahedral positions of neighboring tunnels crossing the structure framework through those non-occupied octahedral sites. The lack of signal in the MAS NMR spectra due to octahedral lithium can be explained considering that a very low population of lithium in the framework octahedra would be enough to allow diffusion in the *a-c* plane, those ions being undetectable. All described results suggest that lithium diffusion along different directions is more complex than that proposed in ref 16, and different hopping rates must be considered for the two types of Li^+ ions.

As stated above and discussed in what follows, proton-exchanged ramsdellite gives some indirect evidence to support the existence of vacancies at the octahedral MO_6 sites (model-I).

Acidity and Proton Conductivity of $\text{H}_2\text{Ti}_3\text{O}_7$. Chemical analyses indicate that the treatment of $\text{Li}_2\text{Ti}_3\text{O}_7$ with nitric acid produces a complete exchange of lithium by proton. The analyses of the exchange solution confirmed that all the lithium was removed from the parent ramsdellite and that its chemical composition is the nominal one. This is because all the lithium ions are accessible for exchange; as demonstrated above, at low temperature (around RT) lithium ions are located inside the tunnels and can easily be removed from there.

The TG analysis of $\text{H}_2\text{Ti}_3\text{O}_7$ showed a 6.5% weight loss in the temperature range 533–823 K. According to reaction 2 this corresponds to the loss of one water molecule to give rutile- TiO_2 ; indeed this is the only product

(27) Aldon, L.; Kubiak, P.; Womes, M.; Jumas, J. C.; Olivier-Fourcade, J.; Tirado, J. L.; Corredor, J. I.; Perez-Vicente, C. *Chem. Mater.* **2004**, *16*, 5721.

(28) <http://sdpd.univ-lemans.fr/powbase/index.html>.

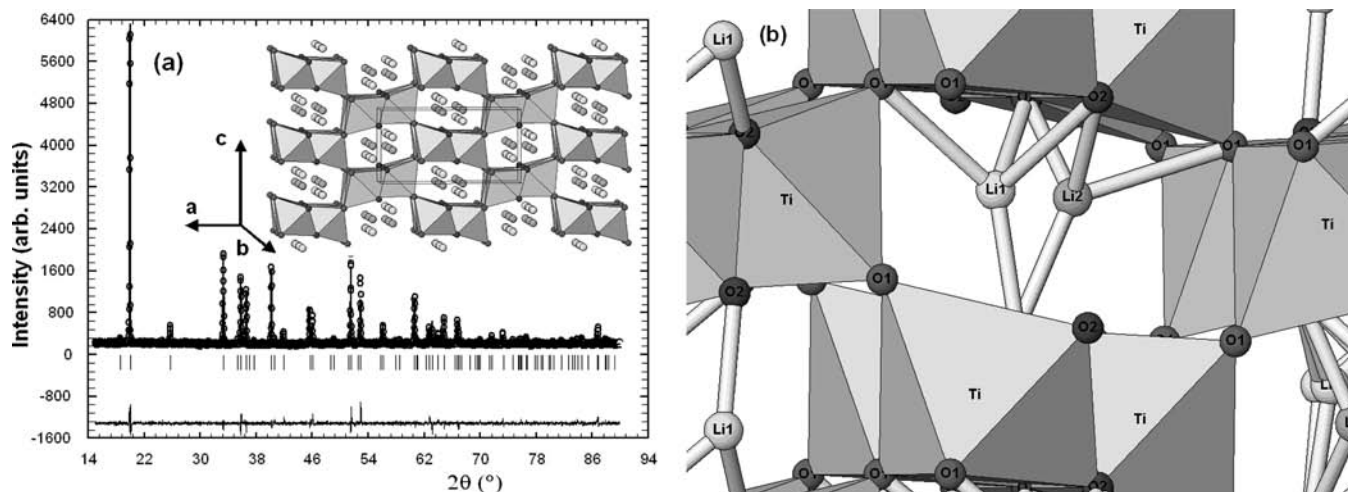


Figure 2. (a) Experimental (points), calculated (solid line), and difference (bottom) XRD patterns recorded at RT for starting ramsdellite $\text{Li}_2\text{Ti}_3\text{O}_7$. In the inset a schematic representation of the ramsdellite structure is shown; (b) Details of the Li coordination polyhedra.

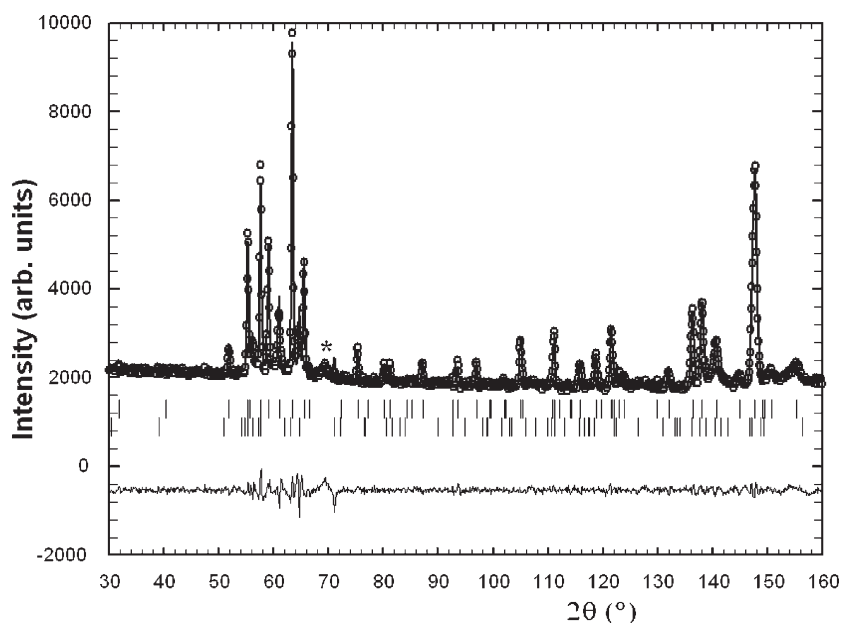
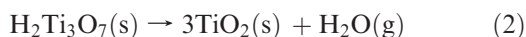


Figure 3. Experimental (points), calculated (solid line), and difference (bottom) NPD patterns of the protonated ramsdellite. The upper row of vertical bars indicates the Bragg peaks of $\text{H}_2\text{Ti}_3\text{O}_7$ (95%), and the peaks corresponding to remaining parent ramsdellite (5%) are indicated by the lower row. The peak labeled by asterisk corresponds to an unknown impurity.

detected in the XRD pattern of the residue (not shown)



In spite of the simplicity of this equation, the release of protons from $\text{H}_2\text{Ti}_3\text{O}_7$ is a complex process as stated in ref 12. Indeed, we observed in our TGA data two mass losses starting at 528 K and 563 K and involving about 40% and 60% of the protons, respectively. This is in good agreement with what reported in ref 12; however, we did not observe any effect in the DTA below 528 K, whereas Le Bail and Fourquet¹² clearly determined the existence of a $\beta\text{-H}_2\text{Ti}_3\text{O}_7$ form between 473 K and 510 K. This suggests that $\alpha\text{-}$ and $\beta\text{-H}_2\text{Ti}_3\text{O}_7$ are energetically very close.

In Figure 3 the graphic result of the fitting of the NPD pattern of the protonated ramsdellite is depicted; the final

structural parameters obtained by the simultaneous fitting of XRD and NPD data are collected in Table 2. Two phases are present in this sample: a major (95%) one of composition $\text{H}_{2.03(1)}\text{Ti}_3\text{O}_7$ and a small amount of the parent compound (5%) which was assumed to have the composition of the initial phase (although it could suffer some degree of exchange). Such a small quantity of lithium remains below the detection limit of chemical analyses. In any case, the lithium-proton exchange was shown to be complete in mild conditions used.

Since neutron scattering power is similar for all atoms, light elements such oxygen, lithium, and hydrogen are easily seen by NPD. As a result of combining XRD and NPD data we ascertained that no vacancies are present in the anionic network, the framework octahedral sites being only occupied by titanium whereas no lithium was detected in the tunnels of proton-exchanged ramsdellite.

Hydrogen atoms were located by Fourier difference synthesis. Their coordinates and population were refined to the final values given in Table 2. Figure 4a shows a schematic representation of the structure of $\text{H}_{2.03(1)}\text{Ti}_3\text{O}_7$; whereas structural details of cation environments are better illustrated in Figure 4b.

Protons are randomly distributed among positions inside the tunnels linked to oxygen atoms (only to O(2)) of the TiO_6 skeleton at a distance of 1.17(2) Å. This distance is longer than that of the covalent bond H–O in water (0.98 Å) but shorter than the corresponding to a hydrogen-bond (1.97 Å). This suggests that protons are strongly bonded to oxygen atoms of the host structure; thus low mobility and poor proton conduction should be expected through a hopping mechanism. However, as NMR and IS results revealed, things are more complex and interesting, as proton conduction is strongly enhanced in wet atmospheres.

The structural model in Table 2 is slightly different of that reported in ref 12; even the unit cells are different: in our case the *a* axis is shorter but the *b* and *c* axes are longer than those reported by Le Bail and Fourquet¹² giving cell volumes of 137.10 Å³ and 133.39 Å³, respectively. The TiO_6 polyhedra are more distorted in our sample (1.882 Å ≤ *d*(Ti–O) ≤ 2.106 Å in our case compared to 1.951 Å ≤ *d*(Ti–O) ≤ 2.02 Å in ref 12). All these differences between the two samples of $\text{H}_2\text{Ti}_3\text{O}_7$ could arise from additional water molecules into the tunnels or from different thermal histories of the samples. The first option in our case is quite unlikely since the sample was always handled under

dry atmosphere and was dried prior to running the NPD experiments. Moreover, no trace of water was found into the tunnels in the Fourier difference maps obtained from NPD. The second option seems more likely, since as reported in ref 12 $\text{H}_2\text{Ti}_3\text{O}_7$ evolves on heating in a very complex way and a $\beta\text{-H}_2\text{Ti}_3\text{O}_7$ phase is formed before protons begin to be removed. Therefore, on heating significant structural changes are expected in such a way that samples submitted to different thermal treatments (for instance to dry the sample) may present subtle differences in their structures.

Interestingly, even the exact location of hydrogen atoms reported in ref 12 is slightly different from the one we observe. We tried this model, but we get a better fit of our NPD data with hydrogen atoms located in the site given in Table 2. In any case, in both models one single crystallographic independent hydrogen atom is present in this material, and the location of H atoms are similar (inside the channels bonded to O(2)); since the data fitting reported in ref 12 and ours give similar agreement factors one can not undoubtedly discard one of the two models proposed.

The ¹H MAS-NMR spectrum of totally proton-exchanged sample, recorded after degassing at 373 K for 2 h, is formed by two components at 9 and 5 ppm, suggesting the existence of two types of hydroxyl groups (Figure 5e).

Proton-exchanged ramsdellite easily absorbs water (this is not the case for the parent $\text{Li}_2\text{Ti}_3\text{O}_7$ ramsdellite); this makes it difficult, and even hinders, the resolution of the two components (see Figure 5). Thus, the as prepared sample, vacuum-dried at 333 K absorbs water from ambient atmosphere, and the corresponding spectrum shows the effect of this absorbed water (Figure 5d): the signal centered at 9 ppm decreases whereas that at 5 ppm remains almost unchanged. For increasing amounts of water, the component at 9 ppm disappears, and the remaining band at 5 ppm shifts towards the position of that of pure water (4.8 ppm) (Figure 5c and b). Further water absorption does not change appreciably the position of this band, but its linewidth significantly decreases, suggesting a progressive increment of proton mobility (Figure 5a).

Table 2. Refined Structure Parameters for Proton-Exchanged $\text{Li}_2\text{Ti}_3\text{O}_7$ Ramsdellite As Obtained by the Simultaneous Fitting of XRD and NPD Data

atom	site ^a	<i>x/a</i>	<i>y/b</i>	<i>z/c</i>	<i>B</i> (Å ²)	occ.
Ti	4c	0.1428(8)	1/4	−0.038(1)	1.20(14)	0.429
O(1)	4c	0.2788(4)	1/4	0.6811(7)	0.44(22)	1/2
O(2)	4c	0.9656(4)	1/4	0.2170(8)	0.44(22)	1/2
H	8d	0.470(3)	0.501(9)	0.094(5)	0.44(22)	0.29(2)

^a S.G. Pnma (62), Composition: $\text{H}_{2.03(2)}\text{Ti}_3\text{O}_7$. The sample contains about 5% of initial $\text{Li}_2\text{Ti}_3\text{O}_7$ ramsdellite; *a* = 9.6951(4) Å, *b* = 2.9591(1) Å, *c* = 4.77909(2) Å, *V* = 137.10(1) Å³. *R*_B = 0.077, *R*_{exp} = 0.017, *R*_{wp} = 0.029, χ^2 = 3.00.

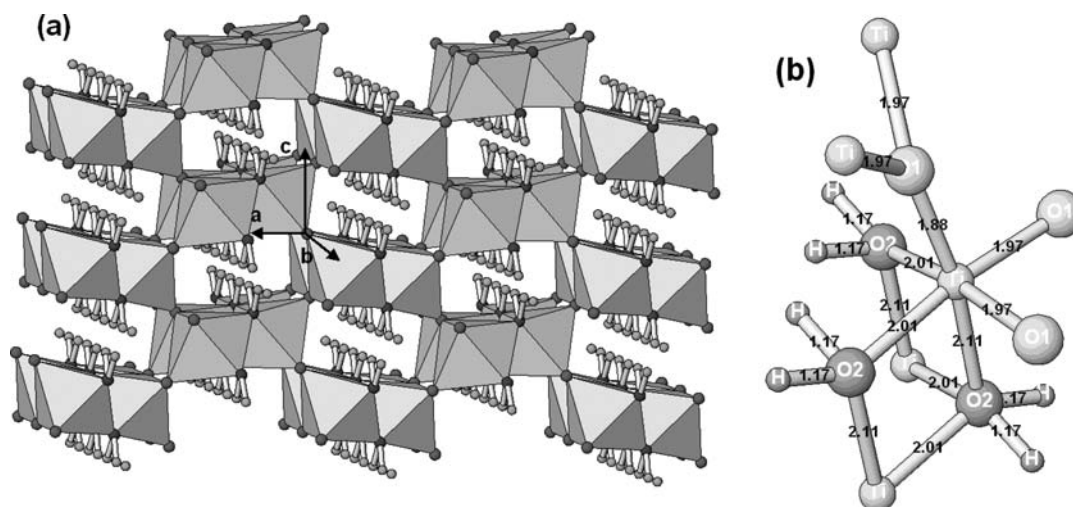


Figure 4. (a) Schematic representation of the structure of $\text{H}_2\text{Ti}_3\text{O}_7$, (b) detail of the atomic environments in $\text{H}_2\text{Ti}_3\text{O}_7$.

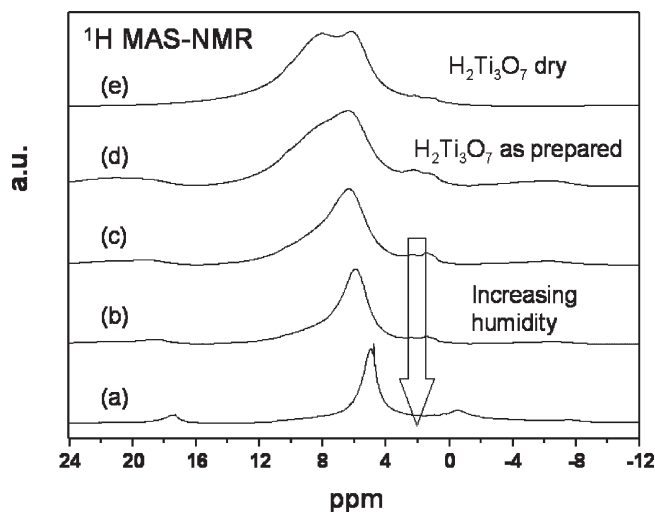


Figure 5. ^1H MAS-NMR spectra of fully protonated $\text{H}_2\text{Ti}_3\text{O}_7$ at different degrees of hydration: (d) as prepared (see text), (e) vacuum dried at 373 K (see text), after exposed to a water-saturated atmosphere at RT for 40 min (c), 120 min (b), and after a week (a).

In the ^1H MAS-NMR spectrum of the exchanged $\text{H}_{2.03(1)}\text{Ti}_3\text{O}_7$ -ramsdellite, differences detected in chemical shift values of two NMR components (Figure 5e) are important, suggesting that the proton charge must be appreciably different in the two OH groups. The presence of two types of OH groups could be thought of as due to protons linked to different oxygen atoms of the structure. However, the refined structural model obtained from NPD (Table 2, Figure 4 and ref 12) rules out this option since H atoms are only bonded to O(2). In ref 13 also two signals are reported in the ^1H -NMR spectrum; these authors claimed that two different H should exist in $\text{H}_2\text{Ti}_3\text{O}_7$.

An alternative explanation for the presence of two signals in the ^1H MAS-NMR spectrum of $\text{H}_2\text{Ti}_3\text{O}_7$ can be derived from the local environments of O(2) atoms to which protons are bonded. Since about 14% of the MO_6 octahedra in the framework are empty (i.e., 0.57 sites over 4 in a unit cell) assuming a random distribution of these vacancies (i.e. no clustering phenomenon would be expected for such a low degree of defects) and taking into account that every M site is coordinated to three O(2) (Figure 4b), two kinds of local environments exist for O(2): $0.57 \times 3 = 1.71$ /unit-cell atoms bonded only to two Ti^{4+} and $4 - 1.71 = 3.43$ /unit-cell O(2) linked to three. This different coordination will produce different electron densities on the O(2) atoms: lower in the latter than in the former. As a final result, the positive charges on the protons linked to these two kinds of O(2) atoms will be also different, giving rise to different NMR signals. We can quantify the population of both types of protons assuming that every O(2) would hold only one H atom; in fact the probability of a given O(2) to be bonded to a proton is only 29%. There are about 43% protons strongly bonded to highly charged O(2) which are coordinated to two Ti^{4+} and a vacancy, for which low acidity is expected. On the other hand, protons linked to low charged O(2) (bonded to three Ti^{4+} ions) amount some 57% and will display a more acidic behavior. Interestingly, the deconvolution (not shown) of spectrum (e) in Figure 5 corresponding to a vacuum-dried sample

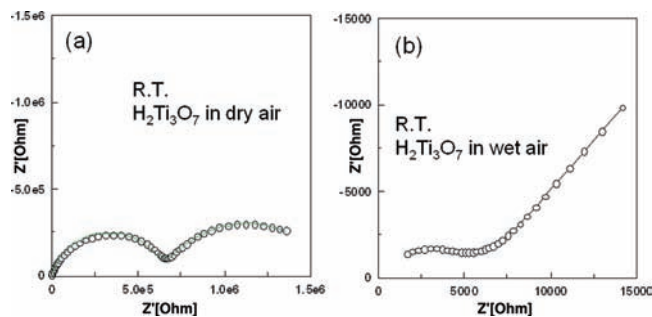


Figure 6. Impedance plots of $\text{H}_2\text{Ti}_3\text{O}_7$ at RT in dry air (a), and in wet air (b).

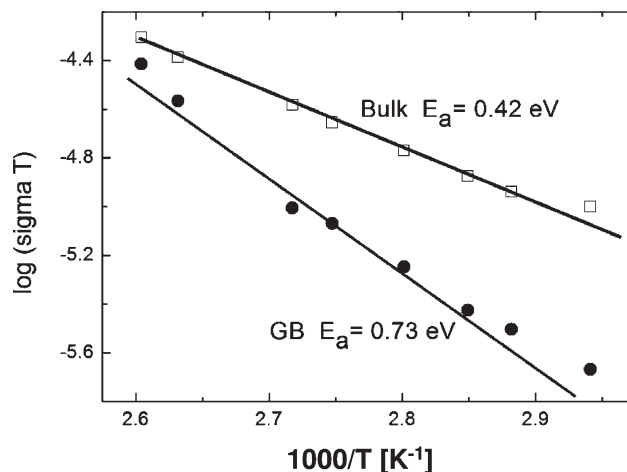


Figure 7. Arrhenius plots for the grain boundary (circles) and bulk contribution (squares) to ionic conduction in $\text{H}_2\text{Ti}_3\text{O}_7$ under dry air.

gives 56% of a signal centered at 8.7 ppm (more acidic proton) and 43% of another one at 6.3 ppm, in very good agreement with the proposed model.

The two detected OH groups display different acidity, as evidenced from ^1H MAS-NMR spectra of hydrated samples. The more acidic protons are easily transferred to water (which acts as a Brønsted alkali); as a result, the signal at 9 ppm decreases as absorbed water increases (Figure 5d and e), and even disappears (Figure 5c). The less acidic protons (signal at 5 ppm) remain unchanged until the amount of absorbed water becomes high (Figure 5a); in this case the ^1H signal shifts towards that of free water and sharpens, indicating an increased proton mobility.

The inherent difficulties to sinter the $\text{H}_2\text{Ti}_3\text{O}_7$ -exchanged material to obtain pellets for conductivity measurements forced the use of high pressure to get compacts. Electrical properties of the so-obtained pellets have been studied at RT both in dry and wet atmospheres. Impedance plots (Figure 6a) of the samples measured under air reveal the existence of two semicircles associated to two electrical responses. The high-frequency semicircle, with capacitance around 5.2×10^{-12} F/cm, can be assigned to the bulk contribution;²⁹ whereas the low frequency one, with capacity about 3.0×10^{-9} F/cm, is related to grain boundaries. The temperature dependence of conductivity was studied on cooling. The grain boundary conductivity

(29) Irvine, J. T. S.; Sinclair, D. C.; West, A. R. *Adv. Mater.* **1990**, 2(3), 132–138.

is smaller than the bulk contribution, (see the Arrhenius plots in Figure 7), with activation energies of 0.73 and 0.42 eV, respectively.

On the other hand, Figure 6b shows the impedance plot of $\text{H}_2\text{Ti}_3\text{O}_7$ measured at RT under wet air. An important change in conductivity is detected for this sample when compared to its behavior under dry conditions (Figure 6a). Ionic conductivity of dry- $\text{H}_2\text{Ti}_3\text{O}_7$ (in a dry atmosphere) at 323 K is as low as $^{323}\sigma_{\text{dry}} \sim 2 \times 10^{-8} (\Omega \text{ cm})^{-1}$; the activation energy for proton diffusion (0.42 eV, Figure 6) being similar to that for lithium ion (0.46 eV);⁴ however, ionic conductivity in $\text{Li}_2\text{Ti}_3\text{O}_7$ is much higher. This could be due to the hopping rate and the site availability factor that are high for lithium in parent ramsdellite⁴ and seem to be very low in the proton-exchanged derivative.

Ionic conductivity in $\text{H}_2\text{Ti}_3\text{O}_7$ increases by six orders of magnitude in a wet atmosphere (water-saturated air at RT). For example, at 323 K conductivity has been found to be now $\sim 2 \times 10^{-2} (\Omega \text{ cm})^{-1}$. ¹H MAS-NMR experiments provided a plausible explanation for this increase in proton mobility. Water molecules enter the tunnels in the structure, since protons in $\text{H}_2\text{Ti}_3\text{O}_7$ are more acidic than water and are transferred to these molecules (see Fig. 5) which provide a vehicle mechanism for proton diffusion. This is an interesting observation that deserves further work to clarify all the structural and mechanistic details of proton migration in this material.

Concluding Remarks

The parallel use of diffraction and spectroscopic techniques to study ramsdellite- $\text{Li}_2\text{Ti}_3\text{O}_7$ support the structural model denoted as $(\text{Li}_{2.29})_c(\text{Ti}_{3.43}\square_{0.57})_f\text{O}_8$ (with all Li tetrahedrally coordinated in the tunnels and some metal vacancies in the MO_6 -octahedra in the framework) instead of the presently accepted one, $(\text{Li}_{1.72})_c(\text{Ti}_{3.43}\text{Li}_{0.57})_f\text{O}_8$ (in which the framework-octahedra are occupied by Li and Ti).

When $\text{Li}_2\text{Ti}_3\text{O}_7$ -ramsdellite is treated with nitric acid a complete exchange of lithium by protons is produced to yield $\text{H}_2\text{Ti}_3\text{O}_7$, confirming previous results.¹² Two kinds of protons are present in this material with different acidity, though all the hydrogen atoms are linked to O(2), being crystallographically equivalent. An explanation of this apparent contradiction can be derived from the local environments of O(2) atoms to which proton are bonded. Two kinds of local environments exist for O(2) inducing different electron densities on them and different acidity for protons: protons strongly bonded to highly charged O(2) (coordinated to two Ti^{4+} and a vacancy) for which low acidity is expected; and protons linked to low charged O(2) (bonded to three Ti^{4+} ions) which will display a more acidic behavior.

Ionic conductivity of dry- $\text{H}_2\text{Ti}_3\text{O}_7$ (in a dry atmosphere) at 323 K is as low as $^{323}\sigma_{\text{dry}} \sim 2 \times 10^{-8} (\Omega \text{ cm})^{-1}$; however, it increases by six orders of magnitude in a wet atmosphere (water-saturated air at RT) $^{323}\sigma_{\text{wet}} \sim 2 \times 10^{-2} (\Omega \text{ cm})^{-1}$. This proton-exchanged ramsdellite absorbs water into the tunnels of the structure. The more acidic protons are easily transferred to water (which acts as a Brønsted alkali) whereas the less acidic protons remain unchanged until the amount of absorbed water becomes important. Proton mobility is enhanced by the presence of absorbed water, explaining the large improvement of electrical conductivity of $\text{H}_2\text{Ti}_3\text{O}_7$ in wet atmospheres. Thus, it seems that water molecules enter the tunnels in the structure providing a vehicle mechanism for proton diffusion.

This makes $\text{H}_2\text{Ti}_3\text{O}_7$ -ramsdellite a potential candidate for hybrid polymeric-inorganic membranes.

Acknowledgment. We would like to thank Ministerio de Educación y Ciencia (project MAT2007-64486-C07) and CAM (program S0505/PPQ0358) for financial support. The access to the neutron facilities at the Laboratoire Léon Brillouin was supported by the ARI action of the HPRI Program of the European Community.